New Aspects on the Mechanism of C_3H_6 Selective Catalytic Reduction of NO in the Presence of O_2 over $LaFe_{1-x}(Cu, Pd)_xO_{3-\delta}$ Perovskites

ARTICLE *in* ENVIRONMENTAL SCIENCE & TECHNOLOGY · SEPTEMBER 2012

Impact Factor: 5.33 · DOI: 10.1021/es302240m · Source: PubMed

5 AUTHORS, INCLUDING:

Biaohua Chen
Beijing University of Chemical Technology

Daniel Duprez
Université de Poitiers

Sebastien Royer
Université de Poitiers

Environmental Science & Technology

Article

pubs.acs.org/est

New Aspects on the Mechanism of C_3H_6 Selective Catalytic Reduction of NO in the Presence of O_2 over $LaFe_{1-x}(Cu, Pd)_xO_{3-\delta}$ Perovskites

Wei Yang,[†] Runduo Zhang,[*,†] Biaohua Chen,[†] Daniel Duprez,[‡] and Sébastien Royer[*,‡]

[†]State Key Laboratory of Chemical Resource Engineering, Beijing University of Chemical Technology, Beijing, 100029, China

[‡]Université de Poitiers, UMR 7285 CNRS, IC2MP, 4 Rue Michel Brunet, Poitiers, 86022 Poitiers Cedex, France

Supporting Information

ABSTRACT: A series of $LaFe_{1-x}(Cu, Pd)_xO_{3-\delta}$ perovskites was fully characterized and tested for the selective catalytic reduction (SCR) of NO by C_3H_6 in the presence of O_2. The adsorbed species and surface reactions were investigated for mechanistic study by means of NO-temperature-programmed desorption (TPD), C_3H_6/O_2-TPD, and in situ diffuse reflectance Fourier transform spectroscopy, in order to discriminate the effects of copper and palladium partial substitutions. With respect to $LaFeO_3$, Cu^{2+} incorporation obviously improved SCR performance, due to its properties for C_3H_6 activation with an easy generation of partially oxidized active surface $C_xH_yO_z$ species. The excellent catalytic activity at the low temperatures over $LaFe_{0.94}Pd_{0.06}O_3$ was attributed to the formation of reactive nitrites/nitrates, leading to a rapid reaction between $adNO_x$ and $C_xH_yO_z$ species, as well as a decreased occupation of the active sites by the inactive ionic nitrates. A mechanism was herein proposed with the formation of nitrite/nitrate and $C_xH_yO_z$ surface species and the further organo nitrogen compounds (ONCs)/−CN/−NCO as important intermediates. Moreover, the acceleration of both formation of inactive ionic nitrate and deep oxidation of C_3H_6 contributed to a negative effect of O_2 excess for NO reduction, while Pd substitution significantly increased the O_2 tolerance ability.

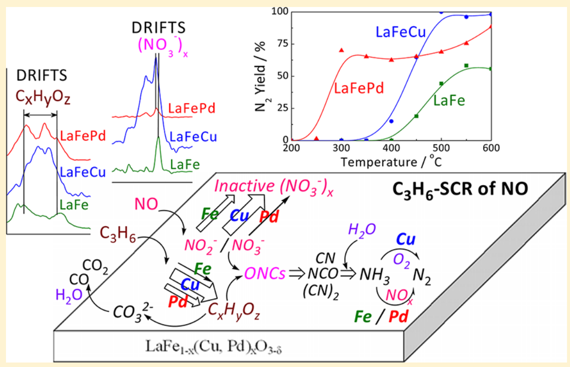

1. INTRODUCTION

The selective catalytic reduction (SCR) of NO by hydrocarbons is a promising method to remove NO_x from automobile exhausts. Various catalytic materials, including ion-exchanged zeolites, supported noble metals, and metal oxides, have been previously investigated for this application. Among them, the limited hydrothermal stability and pore blockage of zeolites restrict their applications, while the low selectivity, easy sintering of active metallic particles, and high cost of supported noble metal catalysts are obviously not suitable for a practically permanent utilization. As a result, metal oxides, including perovskite-type mixed oxides, have attracted much attention due to their high stabilities and durability, low cost, and flexible compositions.[1−4]

Perovskites are mixed oxides with an ABO_3 general formula. Some of the possible compositions (with a lanthanide in the A-position and a transition metal in the B-position) have been proposed to be potential alternatives to the commercial supported noble metals as three-ways catalysts (TWCs) since the beginning of the 1970s,[5] due to their excellent high-temperature thermal and hydrothermal stabilities, great versatility, and excellent redox properties, in addition to a limited cost of the constituting elements. Since the nature of B-site cations, which are commonly the active sites in perovskite, is crucial and decisive for their catalytic performances,[6,7] B-site substitution has been considered to be an effective way to improve their catalytic properties associated with the usual generation of abundant lattice defects, mixed valence states, and oxygen nonstoichiometry.[8] Among the wide variety of B-cations that can partially incorporate the perovskite structure, Cu^{2+} and Pd^{2+} partially substituted into the lattice of nanoscaled Fe-based perovskites synthesized by reactive grinding are found to exhibit a high stability and interesting activity for NO catalytic elimination.[9]

Simultaneously, the SCR mechanism study was widely conducted with different catalysts. On one hand, the SCR process over supported noble metals and some ion-exchanged zeolites has been confirmed, and the hydrocarbon (HC) molecule acts as an oxygen scavenger to restore the initial catalytic site where NO is decomposed.[10−12] On the other hand, a quite distinct mechanism is proposed over many metal oxides or supported non-noble metal catalysts, concluding on a direct interaction between NO_x and HCs. The reaction then proceeds through a series of steps, involving adsorbed nitrogen-containing compounds as the key intermediates toward N_2 formation, depending on the nature of the catalyst.[1,13−23] It should be emphasized that, up to now, the mechanism of NO-

Received: June 5, 2012
Revised: September 16, 2012
Accepted: September 17, 2012
Published: September 17, 2012

   dx.doi.org/10.1021/es302240m | Environ. Sci. Technol. 2012, 46, 11280−11288

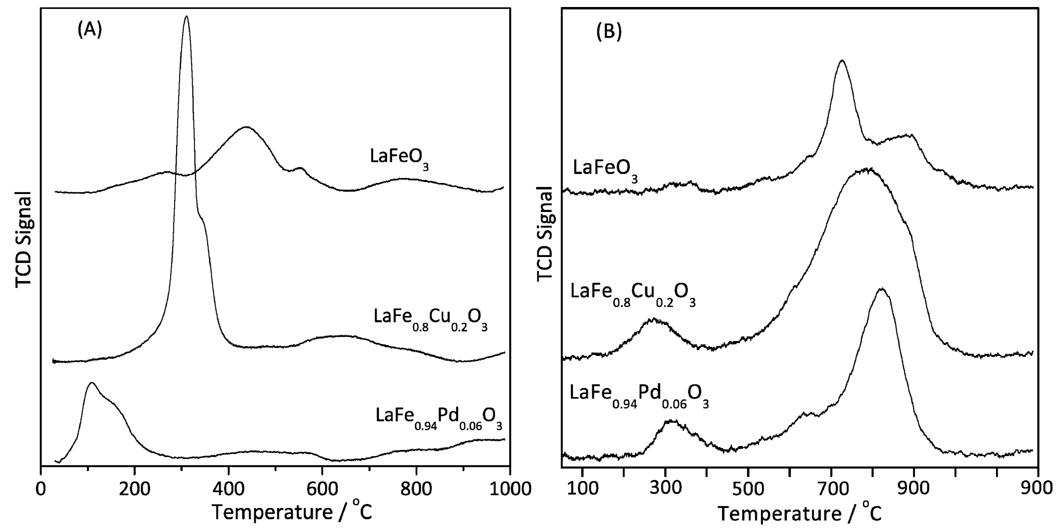

Figure 1. H_2-TPR profiles (A) and O_2-TPD profiles (B) obtained for $LaFe_{1-x}(Cu, Pd)_xO_{3-\delta}$ samples.

SCR by hydrocarbons, especially for the latter one, is still a matter of debate among the catalysis community, while only a few studies are focusing on the NO_x reduction mechanism over perovskites.[9,13]

An effective method for the mechanism analysis is the in situ diffuse reflectance Fourier transform spectroscopy. However, information is still scarce in the literature for perovskite-type catalysts, because of the extremely weak infrared signal due to the poor diffuse reflection ability of perovskites. In this manuscript, the SCR mechanism was carefully studied over $LaFe_{1-x}(Cu, Pd)_xO_{3-\delta}$ catalysts, using DRIFTS and temperature-programmed experiments, aiming at clarifying the correlation between the physicochemical properties and catalytic performance as well as revealing the principle to design an highly active perovskite-type SCR catalyst. The effect of Pd^{2+} or Cu^{2+} substitution and O_2 content on the $deNO_x$ catalytic behaviors was also depicted.

2. EXPERIMENTAL SECTION

2.1. Materials and Characterization. Three ferrite perovskites including $LaFeO_3$, $LaFe_{0.8}Cu_{0.2}O_3$, and $LaFe_{0.94}Pd_{0.06}O_3$ were prepared according to the classical citrate complexation procedure[24] (see details in the Supporting Information, Materials section). Their characterizations of X-ray diffraction (XRD), Brunauer−Emmett−Teller (BET), inductively coupled plasma optical emission spectroscopy (ICP-OES), H_2-temperature-programmed reduction (H_2-TPR), O_2-temperature-programmed desorption (O_2-TPD), NO-TPD, C_3H_6/O_2-TPD, and in situ DRIFTS were accordingly conducted. Prior to TPD tests, the sample was pretreated for 1 h, under a N_2 flow containing 20% O_2 at 550 °C for O_2-TPD, 3000 ppm NO at 500 °C for NO-TPD, or 3000 ppm C_3H_6 and 1% O_2 at 500 °C for C_3H_6/O_2-TPD. (See details in the Supporting Information, Catalyst Characterizations section.)

2.2. Activity Measurement. C_3H_6-SCR of NO was performed in a reaction flow of 100 mL min^{-1} (given a GHSV of ~40 000 h^{-1}), composed of 3000 ppm NO, 3000 ppm C_3H_6, 1% O_2, and balanced with He, over 200 mg of each sample. The effluent gases including NO, C_3H_6, N_2O, NO_2, N_2, NH_3, CO, and CO_2 were online monitored and quantified. (Further details described in the Supporting Information, Activity Measurement section.)

3. RESULTS AND DISCUSSION

3.1. Physicochemical Properties. A perovskite-type structure with an orthorhombic symmetry belonging to the *Pbnm* space group was confirmed by XRD for $LaFe_{1-x}(Cu, Pd)_xO_{3-\delta}$. No diffraction lines corresponding to PdO or CuO can be detected over the substituted samples, suggesting that these cations readily incorporate into the $LaFeO_3$ structure. (See further details in the Supporting Information, Physical and Structural Properties section and Figure S1.) The exact chemical compositions (always close to nominal values), the crystal sizes (D, ranging from 13.7 to 26.4 nm), and surface areas (S_{BET}, varying from 15.4 to 25.3 $m^2 \cdot g^{-1}$) are gathered in Table S1 of the Supporting Information and discussed in the Physical and Structural Properties section.

The results obtained from H_2-TPR show a large difference of redox abilities among the three materials (Figure 1A). Generally, $LaFeO_3$ is detected to be hardly reducible up to 1000 °C, while the incorporation of either Pd or Cu leads to an easier reduction at low temperature, achieving an excellent reducibility at 100 or 300 °C, respectively. However, this reducibility is intimately dependent on the essential nature of substituting cations, which has a limited effect on the reducibility of Fe^{3+} in the perovskite structure. (See detailed description and the results of quantification and calculated values of reduction in the Supporting Information, Redox Properties as Evaluated by H_2-TPR section and Table S2 and Figure S2.)

In order to classify the various oxygen species formed over $LaFe_{1-x}(Cu, Pd)_xO_{3-\delta}$, TPD of O_2 is conducted, as shown in Figure 1B. Over $LaFeO_3$, the O_2 desorption is not intense, and only the oxygen desorption from a few surface monolayers can be observed, which is in accordance with the results obtained by H_2-TPR, confirming a limited reducibility of this structure. After Cu incorporation, surface and lattice O_2 desorption peaks were strongly enhanced. The easier reduction of Cu^{2+} to Cu^0 as well as the vacancies generated in the crystal lattice by Cu^{2+} substitution lead to an easier oxygen diffusion from the bulk to the surface, that is, an increased oxygen mobility. As compared to $LaFeO_3$, the Pd substitution slightly increases the total amount of O_2 desorbed, which may be attributed to the surface oxygen vacancies generated from Pd substitution and the reduction of all the Pd^{2+} ions on the surface or in the bulk. (See detailed description and the results of quantification in the Supporting Information, Oxygen Species as Identified by O_2-TPD section and Table S3.)

3.2. Activity Tests. Figure 2 shows the temperature dependence of N_2 and NH_3 yields for the SCR of NO by

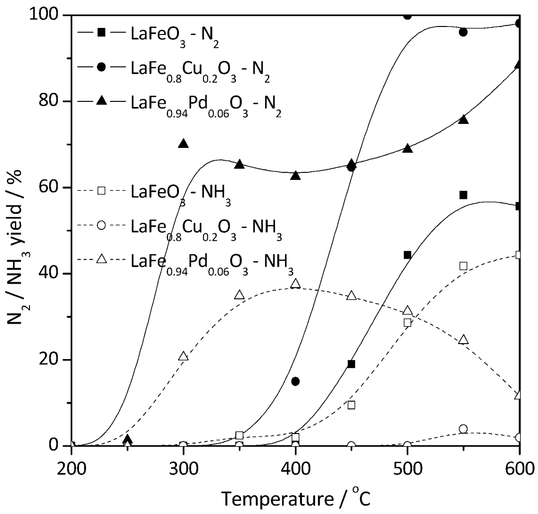

Figure 2. N_2 and NH_3 yields in $C_3H_6/NO/O_2$ reactions over $LaFe_{1-x}(Cu, Pd)_xO_{3-\delta}$ catalysts. Conditions: GHSV = 40 000 h^{-1}, 3000 ppm C_3H_6, 3000 ppm NO, 1% O_2.

C_3H_6 with 1% O_2 over $LaFe_{1-x}(Cu, Pd)_xO_{3-\delta}$. For $LaFeO_3$, the yield of N_2 starts from 450 °C and increases progressively along with temperature up to a maximum of 58% at 550 °C. After Cu substitution, a considerable enhancement is achieved from 400 °C, and the yield of N_2 reaches 98% at 500 °C, which is the maximum value among all the three samples. A remarkable improvement of N_2 yield at low temperature is however observed over $LaFe_{0.94}Pd_{0.06}O_3$, occurring at 250 °C and reaching a value of 68% at 300 °C.

A large amount of NH_3 is detected in the effluents over $LaFeO_3$ and $LaFe_{0.94}Pd_{0.06}O_3$, which is however very limited over $LaFe_{0.8}Cu_{0.2}O_3$. The yield of NH_3 increases progressively up to 44% at 600 °C over $LaFeO_3$, with an initiation at 350 °C. A parabolic yield curve can be seen over $LaFe_{0.94}Pd_{0.06}O_3$ from 300 to 600 °C, reaching a maximum of 37% at 400 °C. For comparison, the NH_3 yield always remains below 4% over the Cu-containing sample. The quantitative analyses of other effluent gases are reported in Figure S3 of the Supporting Information, and the yield of each product as a function of O_2 concentration at 450 °C is presented in Figure S4 of the Supporting Information. The detailed description is addressed in the Supporting Information, Activity Tests section.

3.3. TPD studies of NO and C_3H_6/O_2. *3.3.1. NO-TPD.* As observed in NO-TPD, two NO desorption peaks are clearly observed over each perovskite, which locate at 100−370 °C and above 370 °C (Figure 3A), corresponding to the desorptions of weakly chemisorbed NO species and the thermolysis of surface nitrite/nitrate species, respectively. Pd incorporation obviously declines those high-temperature desorptions, implying a negative effect of the inserted Pd for the accumulation of surface NO_x species. Besides, a significant higher NO/O_2 desorption ratio (above 370 °C) over $LaFeO_3$ could be attributed to the lack of surface O_2 and the poor redox capacity of Fe^{3+} (see further analysis in the Supporting Information, NO-TPD section).

3.3.2. C_3H_6/O_2-TPD. As shown in the C_3H_6/O_2-TPD experiment, C_3H_6 is hardly detected, indicating a weak C_3H_6 chemisorption over the tested samples (Supporting Information, Figure S5B). In Figure 3B, the CO and CO_2 desorptions are observed over $LaFeO_3$ above 200 °C. While the desorption profiles are only slightly modified when palladium incorporates the ferrite structure, desorptions of CO and CO_2 are strongly enhanced over $LaFe_{0.8}Cu_{0.2}O_3$, with a maximum at 400 °C. This result implies that some $C_xH_yO_z$ or carbonate species form on the surface via the adsorption and subsequent oxidation of C_3H_6 and that such a process is obviously promoted by Cu substitution.[13] In fact, when taking into account the larger amount of surface oxygen and higher oxygen mobility in $LaFe_{0.8}Cu_{0.2}O_3$, highly reactive oxygens (surface and bulk) from the solid seem to be beneficial to the oxidation following the steps $C_3H_6 \rightarrow C_xH_yO_z$/carbonates (adsorption−oxidation) → CO/CO_2 (desorbed species). Additionally, it is surmised that the different desorption peaks of CO and CO_2 might be due to

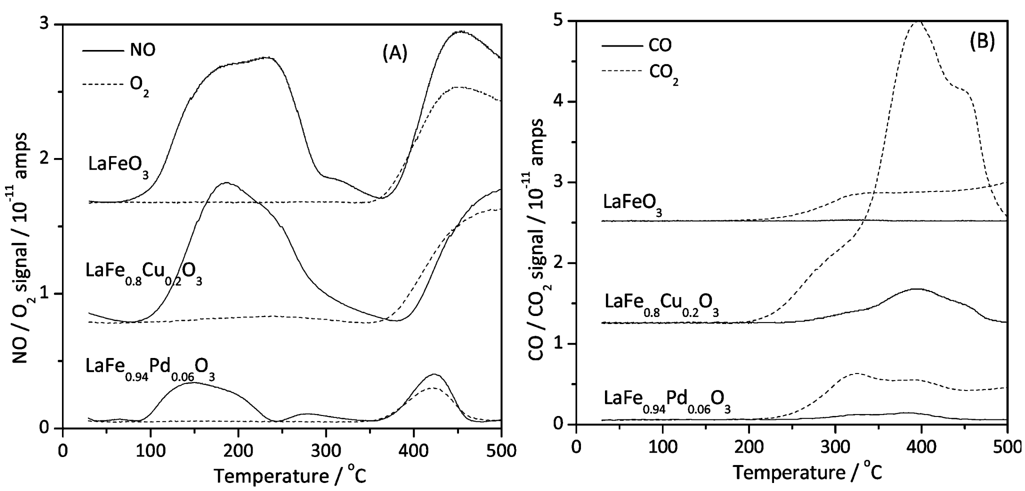

Figure 3. NO- and C_3H_6/O_2-TPD profiles obtained for $LaFe_{1-x}(Cu, Pd)_xO_{3-\delta}$ samples. (A) MS signals recorded for NO and O_2 during NO-TPD. (B) MS signals recorded for CO and CO_2 during C_3H_6/O_2-TPD.

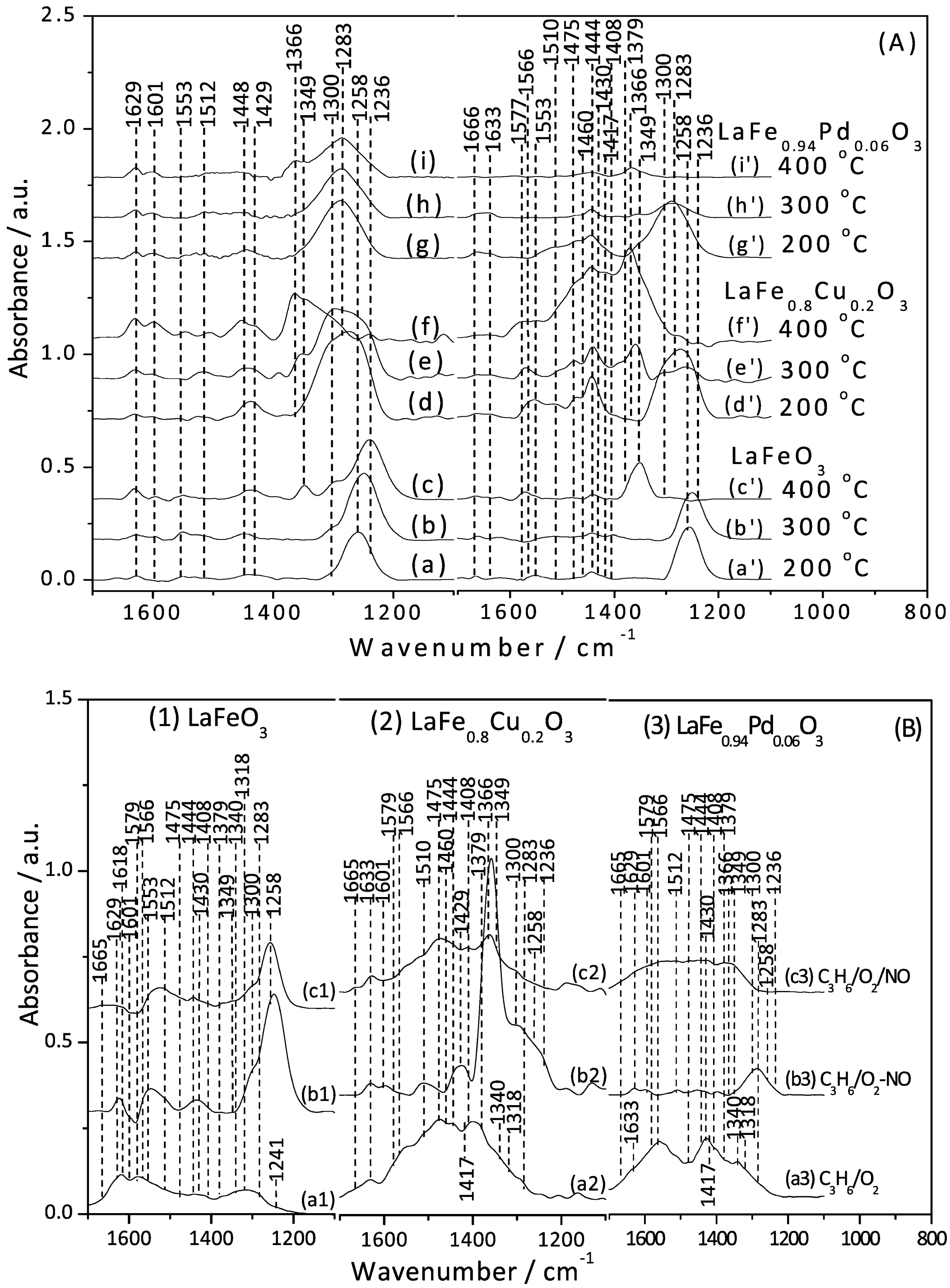

Figure 4. In situ DRIFT spectra: (A) exposure of fresh samples to NO (a–i), followed by C_3H_6/O_2 (a′–i′) at different temperatures; (B) exposure of fresh samples to C_3H_6/O_2 (a1–a3) followed by NO (b1–b3) and to $NO/C_3H_6/O_2$ (c1–c3) at 400 °C. Conditions: NO = 2%; C_3H_6 = 2%; O_2 = 6%; balanced by He. The adsorption time for each step is 15 min.

the desorption of various surface $C_xH_yO_z$/carbonate species exhibiting different thermal stabilities.

3.4. DRIFTS Studies of Stepwise Exposure to NO and/or C_3H_6/O_2. *3.4.1. Adsorption of NO followed by C_3H_6 with O_2 at Different Temperatures on $LaFe_{1-x}(Cu, Pd)_xO_{3-\delta}$.* In order to investigate the surface reactions and intermediates, the various species adsorbed on the surface after exposure to the reactants are studied at different temperatures by means of an in situ DRIFTS experiment. Figure 4A shows in situ IR spectra obtained after exposure to 2% NO in He (Figure 4A, left), followed by 2% C_3H_6 and 6% O_2 in He (NO − C_3H_6/O_2) (Figure 4A, right), at 200, 300, and 400 °C over $LaFe_{1-x}(Cu, Pd)_xO_{3-\delta}$. In the case of $LaFeO_3$, NO flushing at 200 °C produced predominantly linear nitrite NO_2^- species with a band located at 1258 cm^{-1}, with small bands attributable to monodentate nitrate (at 1448 cm^{-1})[14,25] and bridging nitrite species (at 1429 and 1553 cm^{-1}).[26−28] Subsequently, the NO adsorption at higher temperatures (300 or 400 °C) led to a red shift of the intense peak from 1258 to 1236 cm^{-1} gradually, due to the formation of the more stable chelating nitrite instead of linear nitrite.[25−27] Simultaneously, some chelating bidentate nitrate (at 1300 and 1512 cm^{-1})[15,29] and ionic nitrate $Fe^{3+}(NO_3^-)_3$ (at 1349 cm^{-1})[14,25] appear at 300 and 400 °C, respectively. The dominant formation of the nitrite species is consistent to the higher ratio of NO to O_2 obtained during the NO-TPD experiment over $LaFeO_3$. Furthermore, the gas-phase NO_2 signal (at 1601 and 1629 cm^{-1})[29] increases at elevated temperatures (oxidation of NO is considered as the first step in the generation of the nitrite/nitrate-adsorbed species). However, the peak of nitrosyl (adsorbed NO) is not apparent here, which is confirmed by our NO-TPD in Figure 3A and reported to be located at around 1880 cm^{-1} (not shown),[28] due to the overlay of the strong shoulder peaks of gas-phase NO (1760−1960 cm^{-1}). A further introduction of C_3H_6/O_2 leads to a decrease in chelating/linear nitrite and chelating bidentate nitrate signal at 300 °C. Nevertheless, this decrease is likely attributed to the formation and/or to a further desorption of some intermediates rather than the whole SCR process, since NO is not converted at this temperature, as displayed in Figure 2. Surprisingly, these species disappear and transform completely into ionic nitrate at 400 °C even in the absence of NO, attributing to the further oxidation of nitrites and the reformation of nitrates to ionic nitrate.[14,25] Besides, no significant $C_xH_yO_z$ adsorbed species can be detected although C_3H_6 could be converted at 300 and 400 °C, according to the result of the activity test.

In the case of the Cu^{2+}-substituted sample, nearly equally large quantities of linear nitrite and chelating bidentate nitrate (1300 cm^{-1} on Fe^{3+} and 1283 cm^{-1} on Cu^{2+}) form on the surface at 200 °C and decline when temperature increases under NO exposure, while ionic nitrate species on Fe^{3+} [$(NO_3^-)_3$ at 1349 cm^{-1}] and Cu^{2+} [$(NO_3^-)_2$ at 1366 cm^{-1}] form at 300 °C and become dominant at 400 °C. Switching the atmosphere from NO to C_3H_6/O_2 mixture results in the formation of adsorbed $C_xH_yO_z$ species such as formic acid (1379, 1408, 1577 cm^{-1}), acetic acid (1460, 1577 cm^{-1}), and carboxylate (1430, 1510, partial 1379 cm^{-1}), which become visible at 200 °C and accumulate considerably at 400 °C.[1,14,30−33] It is worth noting that the enolic species (RCH═CH—O^-) formed by adsorption of C_3H_6 are also detected at 1633, 1417, and partial 1340 cm^{-1}, which were proposed by He's group to present a much higher activity than formic or acetic acid for NO reduction over Ag/Al_2O_3.[15,19] Actually, organo nitrogen compounds (ONCs), which have been denoted as an intermediate in this reaction sequence, may be reflected by the bands at 1379 and 1408 cm^{-1}.[16] Meanwhile, nitrite/nitrate species are consumed and reform into ionic nitrate, especially at 300 and 400 °C, even more than over pure $LaFeO_3$ sample.

For $LaFe_{0.94}Pd_{0.06}O_3$, the main species on the surface after NO adsorption are chelating bidentate nitrate (1300 cm^{-1} on Fe and 1283 cm^{-1} on Pd) in the temperature range. Ionic nitrate species (1349 cm^{-1} on Fe and 1366 cm^{-1} on Pd) are also detected at the highest temperature (400 °C). Similar to $LaFe_{0.8}Cu_{0.2}O_3$, some $C_xH_yO_z$ adspecies in the range 1400−1550 cm^{-1} appear at low temperature along with a nearly constant amount of adsorbed NO_x. Nitrite/nitrate species are observed to decrease at higher temperature after exposure to C_3H_6/O_2 atmosphere. Nevertheless, the signal for ionic nitrate species decreases at 400 °C, which differs from what occurs over the former two samples.

3.4.2. Adsorption of C_3H_6/O_2 and/or NO at 400 °C on $LaFe_{1-x}(Cu, Pd)_xO_{3-\delta}$. A second DRIFTS experiment is designed to investigate the adsorption/activation of C_3H_6 in the presence of O_2 and to study the reactivity of the adsorbed species toward NO. The reaction, performed at 400 °C, consists in a comparison between the following adsorption processes:

Adsorption of C_3H_6/O_2 (a1−a3 in Figure 4B).

Adsorption of NO following C_3H_6/O_2 (C_3H_6/O_2 − NO, b1−b3 in Figure 4B).

Adsorption of C_3H_6/O_2/NO (c1−c3 in Figure 4B).

Excluding the weak contribution of C_3H_6 in the gas phase with the bands at 1444, 1475, 1629, and 1665 cm^{-1},[14,17] several adsorbed $C_xH_yO_z$ and carbonate species are detected after exposure to C_3H_6/O_2 (Figure 4B, a1−a3). For $LaFeO_3$ (Figure 4B, a1), surface carbonates are found to dominate, with signals from 1240 to 1350 cm^{-1} (at 1241, 1283, 1318, and partial 1340 cm^{-1}, monodentate carbonate), 1550 to 1580 cm^{-1} (at 1566 and 1579 cm^{-1}, chelating carbonate), and an intense band at 1618 cm^{-1} assigned to the hydrogen−carbonates.[14,28,34] Besides, a small amount of enolic species, formic acid, acetic acid, and carboxylate are detected at the same time, and the C−H bending of $-CH_3$ for the adsorbed hydrocarbonates could be reflected by the bands at 1444 and 1475 cm^{-1}. As observed in Figure 4A, f′, a large signal for $C_xH_yO_z$ (at 1408−1633 cm^{-1}, partial 1340 and 1379 cm^{-1}) and carboxylate (at 1510 cm^{-1}) as well as a small signal for carbonate species (at 1283, 1318, and 1566 cm^{-1}) are observed over $LaFe_{0.8}Cu_{0.2}O_3$ (Figure 4B, a2). Importantly, the formation of enolic species (RCH═CH—O^-) formed by adsorption of C_3H_6 is detected to be enhanced for Cu-substituted material. For the Pd-containing material, abundant carbonate and carboxylate species (at 1430 and 1566 cm^{-1}) as well as some $C_xH_yO_z$ coexisted on the surface in the flow of C_3H_6/O_2 (Figure 4B, a3).

Upon switching to 2% NO, the surface $C_xH_yO_z$, carbonate, and carboxylate faded away, accompanied with an increase in the signal of nitrite/nitrate species. $C_xH_yO_z$ amounts declined by reaction with NO, though carbonate and carboxylate species were more likely to decompose directly to CO/CO_2 and O_2. Additionally, nitrite/nitrate species are observed to generate more rapidly over C_3H_6/O_2-treated $LaFeO_3$ and $LaFe_{0.8}Cu_{0.2}O_3$ (Figure 4B, b1,b2) han over the fresh ones (Figure 4A, c,f). This is clearly observed for the ionic nitrate signal growth over $LaFe_{0.8}Cu_{0.2}O_3$ (Figure 4B, b2). This more rapid increase obviously results from the adsorption of O_2 in the previous step. An opposite trend is observed for the Pd-substituted material (Figure 4B, b3), which demonstrates again the different impacts of O_2 on the nitrate generation over different materials, depending on the perovskite composition.

DRIFTS for $NO/C_3H_6/O_2$ coadsorption is performed to further approach to the SCR reaction mechanism over these solids (Figure 4B, c1−c3). Generally speaking, the surface adsorbed species observed were mainly nitrite/nitrate over $LaFeO_3$ (Figure 4B, c1). Considerable amounts of ionic nitrate, $C_xH_yO_z$, and carboxylate species formed over the Cu-containing perovskite (Figure 4B, c2). Meanwhile, comparable amounts of $C_xH_yO_z$, carbonate, carboxylate, and scarce nitrite/nitrate species are generated over the Pd-doped sample (Figure 4B, c3). Obviously, a higher NO conversion of this sample corresponds to a lower accumulation of adNO_x. Furthermore, exposing $LaFeO_3$ to C_3H_6 after NO adsorption led to a rather low concentration of $C_xH_yO_z$ surface species. It can be attributed to a much stronger generation of adNO_x than $C_xH_yO_z$ on this surface, which is indeed disadvantageous to the further deNO_x process. Actually, such a phenomenon may be due to the low redox ability of Fe^{3+} that cannot activate adNO_x for conversion until 400 °C. Some important intermediates produced during the SCR of NO, that is, −NCO, −CN, and adsorbed $(CN)_2$, are also detectable on the surface of these materials, in addition to ONCs. Their direct observation confirms the reaction pathway as proposed in our previous study.[13] Complementary details are presented in the Supporting Information, in the section entitled The Intermediates Observed in DRIFTS Study and in Figure S6.

3.4.3. Correlations between the Results of DRIFTS and Activity Test. It is noticed that the ionic nitrate started to generate at 300 °C (over $LaFe_{0.8}Cu_{0.2}O_3$) or 400 °C (over the other two samples). Cu substitution obviously accelerated the formation of ionic nitrate, while Pd presented a behavior of inhibition on this formation, no matter with or without sufficient O_2. Once generated, such ionic nitrate exhibits good stability and low reactivity in the flow of C_3H_6 reductant, which is obviously not beneficial for the SCR of NO, due to the occupation of reactive sites. Indeed, this could safely contribute to the difference of NO conversion observed between the samples ($LaFe_{0.94}Pd_{0.06}O_3 \gg LaFe_{0.8}Cu_{0.2}O_3$ and $LaFeO_3$) and the tolerance to excess O_2 for SCR of NO ($LaFe_{0.94}Pd_{0.06}O_3 > LaFeO_3 > LaFe_{0.8}Cu_{0.2}O_3$) at the same temperature.

$C_xH_yO_z$ species, especially enolic species, which are commonly considered to be crucial for the successive SCR steps, are found to be more easily produced and to cumulate over $LaFe_{0.8}Cu_{0.2}O_3$ during all the adsorptions involving C_3H_6 ($LaFe_{0.8}Cu_{0.2}O_3 > LaFe_{0.94}Pd_{0.06}O_3 > LaFeO_3$). Compared to $LaFeO_3$, such a significant enhancement over $LaFe_{0.8}Cu_{0.2}O_3$ may facilitate the subsequent formation of intermediates such as ONCs, leading to a higher NO conversion, even though more inactive ionic nitrate generated over this structure at 400 °C. Due to the absence of ionic nitrate on the surface of $LaFe_{0.94}Pd_{0.06}O_3$, more active sites are available; so the moderate improvement of $C_xH_yO_z$ accumulation on this surface may be more effective on NO conversion comparing to $LaFe_{0.8}Cu_{0.2}O_3$.

Likewise, the active nitrite/nitrate species (at 1236−1300 cm^{-1}) are reported to be necessary adspecies available for this reaction, but the easy formation and accumulation of them over all the samples can never be directly related to the difference of NO conversions observed among these solids. Actually, and according to our previous research,[13] Pd incorporation decreased the temperature for the formation of ONCs, while Cu substitution was also beneficial for this process. Pd-substituted solid has the best low temperature redox capability among these active ions. Therefore, the activation of nitrite/nitrate species, including the ionic nitrates, may be favored. A decrease in activation energy necessary for the further interaction between nitrite/nitrate and $C_xH_yO_z$ can be logically awaited. Thus, in addition to the inhibition effect of ionic nitrate, the decrease of the activation energy of the reaction $NO_2^-/NO_3^- + C_xH_yO_z \rightarrow$ ONCs could be treated as another key factor to improve NO conversion, rather than the formation/accumulation of nitrite/nitrate species, over these three catalysts.

3.5. Reaction Pathway. As observed in the activity results, the orders of T_{50} for the N_2 yield, and NO and C_3H_6 conversions are always as follows: $LaFe_{0.94}Pd_{0.06}O_3 < LaFe_{0.8}Cu_{0.2}O_3 < LaFeO_3$, showing a beneficial effect of Pd or Cu incorporation in the perovskite structure for this reaction. According to the adsorbed species detected on the three Fe-based perovskites and the literature about C_3H_6-SCR of NO over different materials,[13,22,30,35] the mechanism of the reaction over $LaFe_{1-x}(Cu, Pd)_xO_{3-\delta}$ can be written involving organo nitrogen compounds and isocyanate/cyanate as intermediate products (Scheme 1).

Scheme 1. Proposed Reaction Pathway for C_3H_6-SCR of NO in the Presence of O_2 over $LaFe_{1-x}(Cu, Pd)_xO_{3-\delta}$

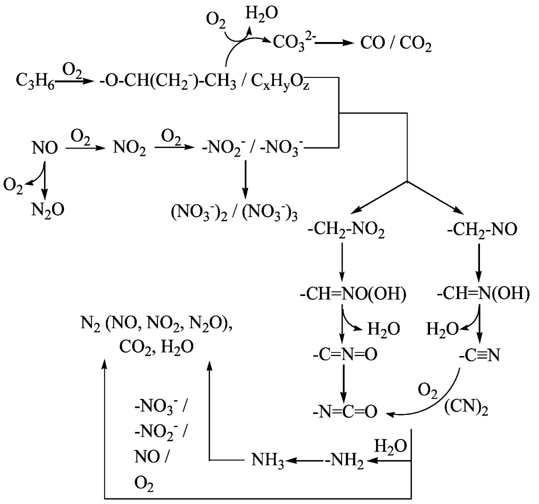

As reported to be two kinds of crucial surface species in the typical C_3H_6-SCR of NO process,[13,35] nitrite/nitrate and $C_xH_yO_z$ are generated initially via the adsorption and the subsequent oxidation of NO and C_3H_6 on the active sites (Fe^{3+}, Cu^{2+}, and Pd^{2+}) (eqs 1 and 2):

$$C_3H_{6(ad)} + O_{2(ad)} \rightarrow -O-CH(CH_2^-)-CH_{3(ad)} \rightarrow C_xH_yO_{z(ad)}\ (\text{enol, } CH_3COOH\text{, HCOOH, HCHO...}) \quad (1)$$

$$NO_{(ad)} + O_{2(ad)} \rightarrow -NO_2^-/-NO_3^-{}_{(ad)} \quad (2)$$

Subsequently, the $C_xH_yO_z$ could be further oxidized by O_2 directly to carbonates and water. The decomposition of carbonates gives rise to CO_2 desorption (eq 3):

$$-O-CH(CH_2^-)-CH_{3(ad)} / C_xH_yO_{z(ad)} + O_{2(ad)} \rightarrow CO_3^{2-}{}_{(ad)} + H_2O \rightarrow CO_{2(g)} \quad (3)$$

As soon as nitrite/nitrate species were formed and activated at higher temperature, $C_xH_yO_z$ was able to react with them to produce N_2, CO_2, and H_2O. Meanwhile, the generation of some byproducts cannot be excluded (eqs 4−7). As a classical SCR of NO sequence described in the literature,[32,35−37] intermediate products (such as ONCs, enolic species, and C_xH_y−CN/−NCO) were indeed detected here by DRIFTS (Supporting Information, Figure S6), showing trace amounts of them on the catalyst surface. This presence in trace is obviously associated with their high reactivity and instability.

$$-O-CH(CH_2^-)-CH_{3(ad)}/C_xH_yO_{z(ad)} + -NO_2^-/-NO_3^-{}_{(ad)} \rightarrow -CH_2-NO_{2(ad)} + -CH_2-NO_{(ad)} \quad (4)$$

$$-CH_2 - NO_{2(ad)} \rightarrow -CH{=}NO(OH)_{(ad)} \rightarrow -CH{=}N{=}O_{(ad)} \rightarrow -N{=}C{=}O_{(ad)} \quad (5)$$

$$-CH_2{-}NO_{(ad)} \rightarrow -CH{=}N(OH)_{(ad)} \rightarrow -C{\equiv}N_{(ad)} \quad (6)$$

$$-CN/-NCO_{(ad)} + NO/-NO_3^-/-NO_2^-{}_{(ad)} \rightarrow N_2\,(NO_2, NO, N_2O)_{(g)} + CO_{2(g)} \quad (7)$$

As another possible intermediate, which was DRIFTS detectable for pure Fe- and Cu-substituted samples (Supporting Information, Figure S6), $(CN)_2$ is easily formed by combination of $C_xH_y{-}CN$ with an assistance of O_2 and further reacts with water through a disproportionation reaction to respectively generate −CN and −NCO (eqs 8 and 9).[38,39] This process cannot be totally excluded after Pd incorporation even if the corresponding specie was not observed, which might react rapidly over Pd^{2+} sites.

$$C_xH_y{-}CN_{ad} + O_{2(ad)} \rightarrow (CN)_{2(ad)} + CO_{2(g)} + H_2O \quad (8)$$

$$(CN)_{2(ad)} + H_2O \rightarrow -CN_{(ad)} + -NCO_{(ad)} \quad (9)$$

It has been thought that the formation of ONCs could be a crucial step in the SCR process.[40,41] Nevertheless, the accurate quantification of these intermediate products is impossible, owing to their rapid transformation, trace amounts, and overlay with bands of other compounds. According to our previous results,[13] the Cu and Pd substitutions have a significantly positive effect on the formation of such organo species, contributing to the improvement in activity.

3.6. Generation of Byproducts: NH_3. Abundant generation of NH_3 accompanying N_2 formation over $LaFeO_3$ and $LaFe_{0.94}Pd_{0.06}O_3$, which becomes much smaller as Cu is incorporated into perovskite lattice, is illustrated in Figure 2. According to the literature, NH_3 could be derived from the hydrolysis of the −CN and −NCO intermediates (eq 10),[35,38,42] after C_3H_6 combustion to satisfy the requirement of water molecules (eq 3). Subsequently, being a well-known reductant for NO and/or NO_2 reductions in the presence of O_2, NH_3 can be converted into N_2 by interacting with the adsorbed NO/nitrite/nitrate or oxygen via normalization or oxidation reaction, with the possible formation of undesirable side products (NO, NO_2, or N_2O) (eq 11):

$$-CN/-NCO_{(ad)} + H_2O \rightarrow NH_{3(g)} + CO/CO_{2(g)} \quad (10)$$

$$NH_{3(ad)} + NO/-NO_3^-/-NO_2^-/O_{2(ad)} \rightarrow N_2(NO_2, NO, N_2O)_{(g)} + H_2O \quad (11)$$

It was reported that iron redox centers presented a considerable capacity of hydrolysis of −CN and −NCO species.[11,38] Meanwhile, lanthanum oxide also promoted this hydrolysis due to its basic properties.[38] These are in favor of LaFe-based perovskites for the elimination of the potential HCN and the successive NO reduction.

In the case of $LaFeO_3$, NH_3 is generated at relatively lower temperature than N_2 does (350 vs 450 °C) (Figure 2), revealing the easier occurrence of hydrolysis (eq 10) as compared to the normalization or oxidation reaction associated with adNO_x species (eqs 7 and 11). Virtually, the appearance of ammonia (at 350 °C) sheds light on the formation of −CN/−NCO or even ONCs, because the hydrolysis reaction is previously reported to occur at rather lower temperatures over Fe, Cu, or Pd redox centers if −CN/−NCO exist.[38,42] Furthermore, the ratio of the generated N_2 and NH_3 achieving over $LaFeO_3$ keeps approximately 1.5 above 450 °C, which is the lowest one among the investigated three perovskites. This illustrates the strong hydrolysis of −CN and −NCO as well as the limited NH_3 reactivity with NO_x or O_2 over pure Fe cores, which could be strongly correlated to the inferior redox capacity of Fe in H_2-TPR and O_2-TPD results.

When Pd is added, the yields of N_2 and NH_3 increase sharply at 300 °C; while the N_2/NH_3 ratio keeps much higher than that over $LaFeO_3$, showing again the strong improvement of Pd substitution on the reaction between NH_3 (or even −NCO/−CN) and NO_x adspecies (mainly as nitrite and nitrate species) with N_2 as the main product, due to the excellent redox capacity of Pd. Moreover, N_2 yield decreases slightly at 350 and 400 °C, corresponding to the intense enhancement of hydrolysis at these temperatures, followed by a promotion of the normalization or oxidation reaction at higher temperatures (eqs 7 and 11).

It has been reported that the Cu-containing catalysts exhibited excellent N_2 selectivity in NH_3 oxidation[43] and HCN hydrolysis[38] in the presence of O_2. Consequently, with a pronounced redox and oxygen mobility properties, Cu-substituted perovskite can be also expected to be an outstanding NH_3 slip catalyst (oxidize NH_3 by O_2) rather than a NH_3-SCR (NH_3 reacts with adNO_x) one. Therefore, the significantly higher selectivity for NO reduction and extremely limited NH_3 emission in the effluent over $LaFe_{0.8}Cu_{0.2}O_3$ can be explained by the easy NH_3 to N_2 selective oxidation and by a potential direct oxidation of −CN/−NCO (eq 12):

$$-CN/-NCO_{(ad)} + O_{2(ad)} \rightarrow N_2(NO_2, NO, N_2O)_{(g)} + CO_{2(g)} \quad (12)$$

In fact, according to the NO total conversion (Supporting Information, Figure S3A), the limited enhancement achieved over $LaFe_{0.8}Cu_{0.2}O_3$ illustrates that the Cu incorporation mainly contributes to the N_2 selectivity rather than the low temperature activity.

In addition to NH_3, CO could be generated through C_3H_6 partial oxidation or −CN hydrolysis (Supporting Information, Figure S3C). Interestingly, the absence of NO_2 during the present activity tests is possibly owing to the high reactivity of NO_2 with NH_3. The small amount of N_2O observed is related to the NO dissociation and the normalization or oxidation reaction (Supporting Information, Figure S3D).

O_2 presents a crucial role in the SCR process (Supporting Information, Figure S4). As a promoter, O_2 can oxidize NO or C_3H_6 into adsorbed nitrite/nitrate or $C_xH_yO_z$ species on the catalyst surface; as an inhibitor, excess of O_2 could consume the reductant and produce inert ionic nitrate species on the surface that depress the adsorption site concentration. This leads to the worst SCR performance of Cu-substituted sample at excess O_2. By contrast, Pd incorporation strongly suppressed the generation of ionic nitrate and enhanced the reactivity of nitrite/nitrate species with $C_xH_xO_z$, giving rise to the best O_2 tolerance.

■ ASSOCIATED CONTENT

Ⓢ Supporting Information

Additional details concerning materials, catalyst characterizations, activity measurement, physical and structural properties, redox properties as evaluated by H_2-TPR, oxygen species as identified by O_2-TPD, activity tests, NO-TPD, the intermediates observed in DRIFTS study, the generation of byproducts: N_2O and CO, and the role of O_2 on catalytic behavior of Fe-based perovskites. This material is available free of charge via the Internet at http://pubs.acs.org.

■ AUTHOR INFORMATION

Corresponding Author

*Phone: +86(0)10-64412054 (R.Z.); +33(0)549453479 (S.R.). Fax: +86(0)10-64419619 (R.Z.); +33(0)549453499 (S.R.). E-mail: zhangrd@mail.buct.edu.cn (R.Z.); sebastien.royer@univ-poitiers.fr (S.R.).

Notes

The authors declare no competing financial interest.

■ ACKNOWLEDGMENTS

The China Scholarship Council (CSC) is acknowledged by W.Y. for its financial support through a one year abroad Ph.D. stay. S.R. acknowledges the CNRS for his six month delegation. R.Z. also thanks the Natural Science Foundation of China (NSFC) under grants no. 20977004, no. 21177008, and no. 21121064 and the New Century Program for Excellent Talents in University (2010-NECT-0204) for the financial support.

■ REFERENCES

(1) Satsuma, A.; Shimizu, K.-I. In situ FT/IR study of selective catalytic reduction of NO over alumina-based catalysts. *Prog. Energy Combust. Sci.* **2003**, *29*, 71−84.

(2) Shelef, M. Selective catalytic reduction of NO_x with N-free reductants. *Chem. Rev.* **1995**, *95* (1), 209−225.

(3) Hamada, H. Selective reduction of NO by hydrocarbons and oxygenated hydrocarbons over metal oxide catalysts. *Catal. Today* **1994**, *22*, 21−40.

(4) Burch, R.; Millington, P. J. Selective reduction of nitrogen oxides by hydrocarbons under lean-burn conditions using supported platinum group metal catalysts. *Catal. Today* **1995**, *26*, 185−206.

(5) Libby, W. F. Promising catalyst for auto exhaust. *Science* **1971**, *171*, 499−500.

(6) Rojas, M. L.; Fierro, J. L. G.; Tejuca, L. G.; Bell, A. T. Preparation and characterization of $LaMn_{1-x}Cu_xO_{3+\lambda}$ perovskite oxides. *J. Catal.* **1990**, *124*, 41−51.

(7) Lisi, L.; Bagnasco, G.; Ciambelli, P.; De Rossi, S.; Porta, P.; Russo, G.; Turco, M. Perovskite-type oxides: II. Redox properties of $LaMn_{1-x}Cu_xO_3$ and $LaCo_{1-x}Cu_xO_3$ and methane catalytic combustion. *J. Solid State Chem.* **1999**, *146*, 176−183.

(8) Porta, P.; De Rossi, S.; Faticanti, M.; Minelli, G.; Pettiti, I.; Lisi, L.; Turco, M. Perovskite-type oxides: I. Structural, magnetic, and morphological properties of $LaMn_{1-x}Cu_xO_3$ and $LaCo_{1-x}Cu_xO_3$ solid solutions with large surface area. *J. Solid State Chem.* **1999**, *146*, 291−304.

(9) Zhang, R. D.; Alamdari, H.; Kaliaguine, S. Water vapor sensitivity of nanosized La(Co, Mn, Fe)$_{1-x}$(Cu, Pd)$_x$O$_3$ perovskites during NO reduction by C_3H_6 in the presence of oxygen. *Appl. Catal., B* **2007**, *72*, 331−341.

(10) Burch, R.; Millington, P. J.; Walker, A. P. Mechanism of the selective reduction of nitrogen monoxide on platinum-based catalysts in the presence of excess oxygen. *Appl. Catal., B* **1994**, *39*, 65−94.

(11) Cant, N. W.; Liu, I. O. Y. The mechanism of the selective reduction of nitrogen oxides by hydrocarbons on zeolite catalysts. *Catal. Today* **2000**, *63*, 133−146.

(12) Rottländer, C.; Andorf, R.; Plog, C.; Krutzsch, B.; Baerns, M. Selective NO reduction by propane and propene over a Pt/ZSM-5 catalyst: a transient study of the reaction mechanism. *Appl. Catal., B* **1996**, *11*, 49−63.

(13) Zhang, R. D.; Villanueva, A.; Alamdari, H.; Kaliaguine, S. Cu- and Pd-substituted nanoscale Fe-based perovskites for selective catalytic reduction of NO by propene. *J. Catal.* **2006**, *237*, 368−380.

(14) Chi, Y.; Chuang, S. S. C. Infrared study of NO adsorption and reduction with C_3H_6 in the presence of O_2 over CuO/Al_2O_3. *J. Catal.* **2000**, *190*, 75−91.

(15) Yu, Y. B.; He, H.; Feng, Q. C.; Gao, H. W.; Yang, X. Mechanism of the selective catalytic reduction of NO_x by C_2H_5OH over Ag/Al_2O_3. *Appl. Catal., B* **2004**, *49*, 159−171.

(16) He, H.; Zhang, C. B.; Yu, Y. B. A comparative study of Ag/Al_2O_3 and Cu/Al_2O_3 catalysts for the selective catalytic reduction of NO by C_3H_6. *Catal. Today* **2004**, *90*, 191−197.

(17) Wan, Y.; Ma, J. X.; Wang, Z.; Zhou, W.; Kaliaguine, S. On the mechanism of selective catalytic reduction of NO by propylene over Cu-Al-MCM-41. *Appl. Catal., B* **2005**, *59*, 235−242.

(18) Joubert, E.; Courtois, X.; Marecot, P.; Canaff, C.; Duprez, D. The chemistry of $DeNO_x$ reactions over Pt/Al_2O_3: The oxime route to N_2 or N_2O. *J. Catal.* **2006**, *243*, 252−262.

(19) Yu, Y. B.; He, H.; Feng, Q. C. Novel enolic surface species formed during partial oxidation of CH_3CHO, C_2H_5OH, and C_3H_6 on Ag/Al_2O_3: an in situ DRIFTS study. *J. Phys. Chem. B* **2003**, *107* (47), 13090−13092.

(20) Bion, N.; Saussey, J.; Haneda, M.; Daturi, M. Study by in situ FTIR spectroscopy of the SCR of NO_x by ethanol on Ag/Al_2O_3—evidence of the role of isocyanate species. *J. Catal.* **2003**, *217*, 47−58.

(21) Jeon, J. Y.; Kim, H. Y.; Woo, S. I. Mechanistic study on the SCR of NO by C_3H_6 over Pt/V/MCM-41. *Appl. Catal., B* **2003**, *44*, 301−310.

(22) Gorce, O.; Baudin, F.; Thomas, C.; Costa, P. D.; Djéga-Mariadassou, G. On the role of organic nitrogen-containing species as intermediates in the hydrocarbon-assisted SCR of NO_x. *Appl. Catal., B* **2004**, *54*, 69−84.

(23) Haneda, M.; Kintaichi, Y.; Inaba, M.; Hamada, H. Infrared study of catalytic reduction of nitrogen monoxide by propene over Ag/TiO_2-ZrO_2. *Catal. Today* **1998**, *42*, 127−135.

(24) Courty, Ph.; Ajot, H.; Marcilly, Ch.; Delmon, B. Oxydes mixtes ou en solution solide sous forme très divisée obtenus par décomposition thermique de précurseurs amorphes. *Powder Technol.* **1973**, *7*, 21−38.

(25) Liu, L. J.; Chen, Y.; Dong, L. H.; Zhu, J.; Wan, H. Q.; Liu, B.; Zhao, B.; Zhu, H. Y.; Sun, K. Q.; Dong, L.; Chen, Y. Investigation of the NO removal by CO on $CuO-CoO_x$ binary metal oxides supported on $Ce_{0.67}Zr_{0.33}O_2$. *Appl. Catal., B* **2009**, *90*, 105−114.

(26) Zhang, F. X.; Zhang, S. J.; Guan, N.; Schreier, E.; Richter, M.; Eckelt, R.; Fricke, R. NO SCR with propane and propene on Co-based alumina catalysts prepared by co-precipitation. *Appl. Catal., B* **2007**, *73*, 209−219.

(27) Qi, G. S.; Yang, R. T. MnO_x-CeO_2 mixed oxides prepared by co-precipitation for selective catalytic reduction of NO with NH_3 at low temperatures. *Appl. Catal. B* **2004**, *51*, 93−106.

(28) Zhang, R. D.; Teoh, W. Y.; Amal, R.; Chen, B. H.; Kaliaguine, S. Catalytic reduction of NO by CO over $Cu/Ce_xZr_{1-x}O_2$ prepared by flame synthesis. *J. Catal.* **2010**, *272*, 210−219.

(29) Stasio, S. D.; Santo, V. D. DRIFTS study of surface reactivity to NO_2 by zinc nanoparticle aggregates and zinc hollow nanofibers. *Appl. Surf. Sci.* **2006**, *253*, 2899−2910.

(30) Yu, Y. B.; Zhang, X. L.; He, H. Evidence for the formation, isomerization and decomposition of organo-nitrite and -nitro species during the NO_x reduction by C_3H_6 on Ag/Al_2O_3. *Appl. Catal., B* **2007**, *75*, 298−302.

(31) Shimizu, K.; Kawabata, H.; Satsuma, A.; Hattori, T. Role of acetate and nitrates in theselective catalytic reduction of NO by propene over alumina catalyst as investigated by FTIR. *J. Phys. Chem. B* **1999**, *103*, 5240−5245.

(32) Zuzaniuk, V.; Meunier, F. C.; Ross, J. R. H. Differences in the reactivity of organo-nitro and nitrito compounds over Al_2O_3-based catalysts active for the selective reduction of NO_x. *J. Catal.* **2001**, *202*, 340−353.

(33) Hornés, A.; Bera, P.; Cámara, A. L.; Gamarra, D.; Munuera, G.; Martínez-Arias, A. CO-TPR-DRIFTS-MS in situ study of CuO/$Ce_{1-x}Tb_xO_{2-y}$ (x = 0, 0.2 and 0.5) catalysts: Support effects on redox properties and CO oxidation catalysis. *J. Catal.* **2009**, *268*, 367−375.

(34) Venkov, T.; Hadjiivanov, K.; Milushev, A.; Klissurski, D. Fourier transform infrared spectroscopy study of the nature and reactivity of NO_x compounds formed after coadsorption of NO and O_2 on Cu/ZrO_2. *Langmuir* **2003**, *19*, 3323−3332.

(35) Meunier, F. C.; Breen, J. P.; Zuzaniuk, V.; Olsson, M.; Ross, J. R. H. Mechanistic aspects of the selective reduction of NO by propene over alumina and silver−alumina catalysts. *J. Catal.* **1999**, *187*, 493−505.

(36) Cowan, A. D.; Cant, N. W.; Haynes, B. S.; Nelson, P. F. The catalytic chemistry of nitromethane over Co-ZSM5 and other catalysts in connection with the methane-NO_x SCR reaction. *J. Catal.* **1998**, *176*, 329−343.

(37) Obuchi, A.; Wogerbauer, C.; Köppel, R.; Baiker, A. Reactivity of nitrogen containing organic intermediates in the selective catalytic reduction of NO_x with organic compounds: a model study with *tert*-butyl substituted nitrogen compounds. *Appl. Catal., B* **1998**, *19*, 9−22.

(38) Kröcher, O.; Elsener, M. Hydrolysis and oxidation of gaseous HCN over heterogeneous catalysts. *Appl. Catal., B* **2009**, *92*, 75−89.

(39) Janz, G. J.; Woodburn, H. M.; Pecka, J. T.; Dolce, T. J. Cyanogen. In *Inorganic Syntheses*; Moeller, T., Ed.; John Wiley & Sons, Inc.: Hoboken, NJ, 2007; Vol. *5*, pp 43−48.

(40) Iwasawa, Y.; Smits, R. H. H. Reaction mechanisms for the reduction of nitric oxide by hydrocarbons on Cu-ZSM-5 and related catalysts. *Appl. Catal., B* **1995**, *6* (3), 201−207.

(41) Yokoyama, C.; Misono, M. Catalytic reduction of nitrogen oxides by propene in the presence of oxygen over cerium ion-exchanged zeolites: II. Mechanistic study of roles of oxygen and doped metals. *J. Catal.* **1994**, *150*, 9−17.

(42) Cant, N. W.; Chambers, D. C.; Liu, I. O. Y. The formation of isocyanic acid and ammonia during the reduction of NO over supported platinum group metals. *Catal. Today* **2004**, *93*−*95*, 761−768.

(43) Yang, M.; Wu, C. Q.; Zhang, C. B.; He, H. Selective oxidation of ammonia over copper-silver-based catalysts. *Catal. Today* **2004**, *90*, 263−267.